AEDC-TR-66-194

Cy 1

MACH 8 AERODYNAMIC AND AEROTHERMODYNAMIC CHARACTERISTICS OF THE NIMBUS B SPACECRAFT AND SNAP-19 NUCLEAR GENERATOR

R. H. Burt

ARO, Inc.

October 1966

VON KÁRMÁN GAS DYNAMICS FACILITY
ARNOLD ENGINEERING DEVELOPMENT CENTER
AIR FORCE SYSTEMS COMMAND
ARNOLD AIR FORCE STATION, TENNESSEE

NOTICES

MACH 8 AERODYNAMIC AND AEROTHERMODYNAMIC CHARACTERISTICS OF THE NIMBUS B SPACECRAFT AND SNAP-19 NUCLEAR GENERATOR

R. H. Burt
ARO, Inc.

FOREWORD

The work reported herein was done at the request of the Atomic Energy Commission (AEC) for the Martin Company, Baltimore Division, under the AEC SNAP-19 Program, AEC Activity Number 04-60-50-01.1.

The results of the tests presented were obtained by ARO, Inc. (a subsidiary of Sverdrup & Parcel and Associates, Inc.), contract operator of the Arnold Engineering Development Center (AEDC), Air Force Systems Command (AFSC), Arnold Air Force Station, Tennessee, under Contract AF40(600)-1200. The tests were conducted from June 15 to July 16, 1966, under ARO Project No. VT1682, and the manuscript was submitted for publication on September 13, 1966.

This technical report has been reviewed and is approved.

Donald E. Beitsch
Major, USAF
AF Representative, VKF
Directorate of Test

Leonard T. Glaser
Colonel, USAF
Director of Test

ABSTRACT

Static-stability and axial-force characteristics were obtained on a 10-percent scale model of the Nimbus B spacecraft and on a 30-percent scale model of the SNAP-19 nuclear generator at angles of attack from 0 to 180 deg and model roll angles from 0 to 225 deg on the Nimbus and from -60 to 270 deg on the SNAP-19 models. Heat-transfer distributions were obtained on three 30-percent scale models of the SNAP-19 generator with various fin lengths to simulate fin ablation and at angles of attack from 0 to 90 deg and model roll angles of 0 and 30 deg. The tests were conducted at Mach 8 at a free-stream Reynolds number of 0.4 million per foot. Selected results are presented to illustrate the types of data obtained.

CONTENTS

		Page
	ABSTRACT	iii
	NOMENCLATURE	vi
I.	INTRODUCTION	1
II.	APPARATUS	
	2.1 Wind Tunnel	1
	2.2 Models and Support	2
	2.3 Instrumentation	3
III.	PROCEDURE	
	3.1 Test Procedure	4
	3.2 Data Reduction	4
IV.	RESULTS AND DISCUSSION	
	4.1 Nimbus Force Test	5
	4.2 SNAP-19 Force Test	5
	4.3 SNAP-19 Heat-Transfer Test	5

ILLUSTRATIONS

Figure		
1.	Nimbus Spacecraft Model	
	a. Model Details	7
	b. Photograph Showing Model and Components	8
	c. Photograph of Assembled Model, δ = 60 deg.	9
	d. Photograph Showing the Solar Paddles Folded	10
	e. Photograph Showing Sensory Ring-SNAP-19 Configuration	11
2.	SNAP-19 Force Model	
	a. Model Details	12
	b. Photograph of Model and Components	13
3.	SNAP-19 Heat-Transfer Models	
	a. Model Details	14
	b. Photograph of Models	15
4.	Typical Schlieren Photographs of Nimbus Model	
	a. α_S = 45 deg, ϕ_M = 0, δ = +90 deg	16
	b. α_S = 159 deg, ϕ_M = 180 deg, δ = -60 deg	17

Figure		Page
5.	Aerodynamic Characteristics of the Nimbus Spacecraft with Insulation Blankets Off, $\delta = 0$	
	a. Longitudinal Stability and Axial Force	18
	b. Lateral Stability and Rolling Moment	19
6.	Aerodynamic Characteristics of the SNAP-19 Generator with Nonablated Fins	
	a. Longitudinal Stability and Axial Force	20
	b. Lateral Stability and Rolling Moment	21
7.	Heat-Transfer Distributions on the SNAP-19 Generator with Nonablated Fins	
	a. Centerbody	22
	b. Fins	23

NOMENCLATURE

b	Model skin thickness, ft
C_{A_t}	Total axial-force coefficient, total axial force/$q_\infty S$
C_ℓ	Rolling-moment coefficient about model centerline, rolling moment/$q_\infty S L$
C_m	Pitching-moment coefficient about model moment reference points (see Figs. 1a and 2a), pitching moment/$q_\infty SL$
C_N	Normal-force coefficient, normal force/$q_\infty S$
C_n	Yawing-moment coefficient about model moment reference points (see Figs. 1a and 2a), yawing moment/$q_\infty S L$
C_Y	Side-force coefficient, side force/$q_\infty S$
c	Specific heat of model skin material, Btu/lb_m-°R
c_{p_o}	Specific heat of air at stilling chamber conditions, Btu/lb_m-°R
H_o	Enthalpy of air evaluated at stilling chamber conditions, Btu/lb_m
H_w	Enthalpy of air evaluated at model wall conditions, Btu/lb_m
L	Model reference lengths (see Figs. 1a and 2a), in.
M_∞	Free-stream Mach number
p_o	Stilling chamber pressure, psia
$\dot{q}$	Aerodynamic heat-transfer rate, Btu/ft^2-sec

q_∞	Free-stream dynamic pressure, psia
Re_∞	Free-stream unit Reynolds number, ft^{-1}
S	Model reference areas (see Figs. 1a and 2a), $in.^2$
St	Stanton number
St_{ref}	Theoretical stagnation Stanton number of a 1.22-in.-radius hemisphere
T_o	Stilling chamber temperature, °R
T_w	Model wall temperature, °R
t	Time, sec
u_∞	Free-stream velocity, ft/sec
w	Density of model material, lb_m/ft^3
x	Axial distance along model centerline, in.
α_s	Model angle of attack (independent of model roll angle), deg
δ	Solar paddle deflection angle (see Fig. 1a), deg
ϕ_M	Model roll angle about model axis, deg
ρ_∞	Free-stream density, lb_m/ft^3

SECTION I
INTRODUCTION

The objective of the present tests was to obtain aerodynamic and aerothermodynamic data on the Nimbus B spacecraft and SNAP-19 nuclear generator. The stability and axial-force data will be used in a 6-deg of freedom computer program to predict the trajectory and motion-time history of the vehicles during earth re-entry. The aerodynamic heating data will be used with these results to analyze the mode of destruction of the spacecraft and generator to confirm the safety of the system.

The tests were conducted in three phases. During the first phase, the static-stability characteristics of various configurations of a 10-percent scale model of the Nimbus B spacecraft were obtained. Solar paddle positions were varied, the effect of sensory ring insulation blankets was determined, solar paddle bending moments were obtained, and a configuration consisting of only the sensory ring and SNAP-19 was tested. These configurations were tested at angles of attack from 0 to 180 deg and model roll angles of 0, 45, 90, 180, and 225 deg. During the second phase, the static-stability and axial-force characteristics of a 30-percent scale model of the SNAP-19 generator were obtained at angles of attack from 0 to 180 deg and model roll angles from -60 to 270 deg. The effect of shorter fins, to simulate fin ablation, was also determined. During the third phase, heat-transfer distributions were obtained on three 30-percent scale models of the SNAP-19 generator at angles of attack from 0 to 90 deg and model roll angles of 0 and 30 deg. Each model had different length fins to simulate various degrees of fin ablation.

The tests were conducted in the 50-in. hypersonic tunnel (Gas Dynamic Wind Tunnel, Hypersonic (B)) at Mach 8 and a free-stream unit Reynolds number of 0.4 million per foot. The heat-transfer model with the shortest fins was also tested at a unit Reynolds number of 1.5 million per foot.

SECTION II
APPARATUS

2.1 WIND TUNNEL

Tunnel B is a continuous, closed-circuit, variable density wind tunnel with an axisymmetric contoured nozzle and a 50-in.-diam test

section. The tunnel operates at a nominal Mach number of 6 or 8 at stagnation pressures from 20 to 280 and from 50 to 900 psia, respectively, at stagnation temperatures up to 1350°R. The model may be injected into the tunnel for a test run and then retracted for model cooling or model changes without interrupting the tunnel flow. A description of the tunnel may be found in the Test Facilities Handbook[1].

2.2 MODELS AND SUPPORT

2.2.1 Nimbus Force Model

A 10-percent scale, stainless steel model of the Nimbus Spacecraft was furnished by the Martin Company. A sketch of the complete model and photographs of the model components and various configurations are shown in Fig. 1. Several interchangeable parts were used in order to cover an angle-of-attack range from 0 to 180 deg with roll angles of 0, 45, 90, 180, and 225 deg. A photograph showing all the components used in this phase of the test is shown in Fig. 1b. The angle-of-attack range was covered by attaching the balance to either the control housing ($0 < \alpha_s < 90$ deg) or sensory ring ($90 < \alpha_s < 180$ deg). Model roll angles were obtained by rolling the model on prebend adapters between the balance and model. Windshields were used to prevent the airstream from impinging directly on the balance water jacket.

The solar paddles were mounted on flanges so that the paddle deflection, δ, could be changed in 30-deg increments. Using this scheme, configurations with paddles off and deflections of 0, ±30, ±60, and +90 deg (see Figs. 1a and c) were obtained. A configuration with the paddles folded was obtained by replacing the paddles with a separate component as shown in Fig. 1d. A configuration consisting of the sensory ring and the SNAP-19 was a separate model (see Fig. 1e).

The sensory ring on each configuration had an open area, as noted in Fig. 1a, which could be closed by installing steel plates which simulated insulation blankets. These blankets were 0.20 in. thick and were installed on both the front and back sides of the sensory ring.

2.2.2 SNAP-19 Force Model

A sketch of the 30-percent scale, stainless steel model of the SNAP-19 generator and photographs of the model and components are

[1]Test Facilities Handbook (5th Edition). "von Kármán Gas Dynamics Facility, Vol. 4." Arnold Engineering Development Center, July 1963.

shown in Fig. 2. Two rays of fins were interchangeable with shorter fins in order to determine the effect of ablated fins on the aerodynamic characteristics of the model.

2.2.3 SNAP-19 Heat-Transfer Models

The 30-percent scale, stainless steel heat-transfer models were of thin-skin type of construction. Each model had different fin lengths, as shown in Fig. 3, to simulate various degrees of fin ablation. Thermocouples were located along three fins, the centerbody, and the nose. The model with the shortest fins had 78 thermocouples, whereas the other two models had 98 thermocouples each.

2.3 INSTRUMENTATION

2.3.1 Force Tests

Model forces and moments were measured with two six-component, moment-type, strain-gage balances supplied and calibrated by VKF. Before the tests, combined balance static loadings were applied, simulating the model loading range anticipated during the tests. The uncertainties listed below correspond to the differences between the applied loads and the values calculated by the final data reduction balance equations.

Balance Component	Design Load		Maximum Static Loads		Uncertainties	
	Nimbus	SNAP-19	Nimbus	SNAP-19	Nimbus	SNAP-19
Normal force, lb	400	80	80	20	±0.36	±0.21
Pitching moment, in.-lb	1400	300	330	40	±1.82	±0.52
Side force, lb	200	80	40	20	±0.30	±0.16
Yawing moment, in.-lb	700	300	160	40	±1.65	±0.54
Rolling moment, in.-lb	50	25	100	10	±0.68	±0.09
Axial force, lb	50	30	50	20	±0.15	±0.13

Bending moments on the Nimbus paddle supports were measured with two full bridges of high temperature strain gages. The gages were installed on the supporting rod inside the control housing by the Martin Company and calibrated by VKF. The bending-moment data were subject to temperature zero-shifts during a run and are being analyzed by the Martin Company.

2.3.2 Heat-Transfer Tests

The heat-transfer model surface temperature was measured with thermocouples welded to the model inner surfaces and fin leeward surfaces. Thermocouple outputs were recorded on magnetic tape, at a rate of 20 times per second, from the start of the injection cycle until about 5 sec after the model reached the tunnel centerline. From calibrations of a typical thermocouple wire and a knowledge of the system sensitivity and noise level, the precision of the VKF temperature recording system is estimated to have been ±0.2°R/sec or ±2 percent, whichever was greater.

Model flow field schlieren photographs were obtained during all tests. Figure 4 shows typical photographs.

SECTION III
PROCEDURE

3.1 TEST PROCEDURE

The tests were conducted at the following conditions:

M_∞	p_o, psia	T_o, °R	q_∞, psia	$Re_\infty \times 10^{-6}$ ft^{-1}
7.86	70	1170	0.35	0.4
7.95	300	1270	1.42	1.5

All models were tested at the first test condition, and in addition, one heat-transfer model (Configuration 3, Fig. 3d) was tested at the second test condition.

3.2 DATA REDUCTION

Aerodynamic heating rates were calculated using temperature-time data in the relation

$$\dot{q} = wbc\, dT_w/dt$$

which neglects conduction and radiation losses. An evaluation of the specific heat, c, of a sample of the model material, Inconel 600, indicated that c was constant, 0.113 Btu/lb_m-°R, up to a temperature of 760°R which was higher than the maximum model temperature encountered during the tests. The density, w, of the model material was 526 lb_m/ft^3.

The heat-transfer data presented in this report were evaluated at t = 0.25 sec after the model reached tunnel centerline. At this time the model flow field was well established, and conduction errors were minimum.

Stanton numbers were computed from the relation $St = \dot{q}/\rho_\infty u_\infty(H_O - H_W)$. These values were then normalized by a theoretical Stanton number, St_{ref}, computed from the Fay and Riddell theory for the stagnation point of a sphere having the same radius as the generator end plate (1.22 in.).

SECTION IV
RESULTS AND DISCUSSION

4.1 NIMBUS FORCE TEST

The aerodynamic characteristics of the Nimbus spacecraft without insulation blankets and with zero solar paddle deflection ($\delta = 0$) are shown in Fig. 5. The longitudinal stability data presented in Fig. 5a show that this configuration had a stable trim point at $\alpha_S = 0$ for $\phi_M = 0$ and 45 deg. Decreases in the magnitude of CA_t occurred at $50 < \alpha_S < 170$ deg with increasing ϕ_M caused by the SNAP-19 becoming less windward. Lateral stability characteristics are shown in Fig. 5b. Large negative rolling moments were obtained near $\alpha_S = 75$ and 280 deg with $\phi_M = 45$ deg.

4.2 SNAP-19 FORCE TEST

The aerodynamic characteristics of the SNAP-19 generator with nonablated fins are shown in Fig. 6. The longitudinal stability data for this configuration, Fig. 6a, indicate stable trim points for $\phi_M = 0$ at angles of attack of approximately 20, 80, and 280 deg. Model roll angles of 45 and 90 deg resulted in relatively large rolling moments as shown in Fig. 6b.

4.3 SNAP-19 HEAT-TRANSFER TEST

Typical heat-transfer distributions on the SNAP-19 generator centerbody with nonablated fins are shown in Fig. 7a. The upper portion of the figure shows that the maximum heat rate along this ray of the centerbody occurred at x = 5.7 in. and at $\alpha_S = 30$ deg. The magnitude of

the maximum rate was 1.7 times the theoretical stagnation heating rate on a 1.22-in.-radius hemisphere. The data at this model station, $x \approx 5.7$ in., are crossplotted in the lower portion of Fig. 7a to illustrate the effect of model roll angle. At $\alpha_S = 30$ deg, the maximum rate at this model station increased to 2.3 times the stagnation rate as the model was rolled to $\phi_M = 30$ deg.

Heat-transfer distribution along a fin on this configuration at $\phi_M \approx 0$ is presented in Fig. 7b. At $\alpha_S = 0$, heating rates up to 5.4 times the reference hemisphere stagnation value were obtained near the leading edge of the front fin. This value is indicative of the stagnation point heating rate on the fin since the thermocouple was located only 0.10 in. from the leading edge. The maximum heating rates on the rear fin were approximately 2.5 times the reference hemisphere stagnation value.

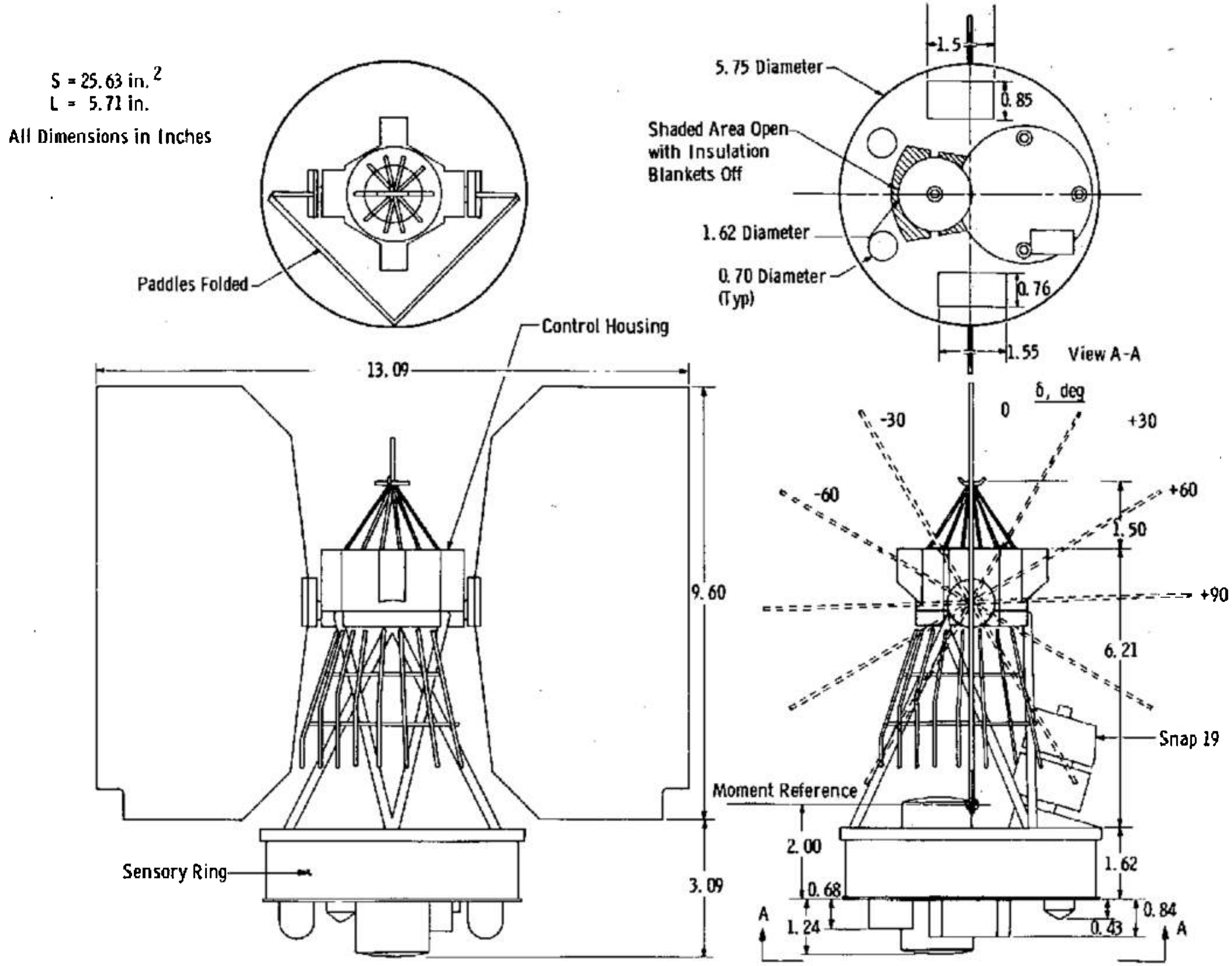

a. Model Details

Fig. 1 Nimbus Spacecraft Model

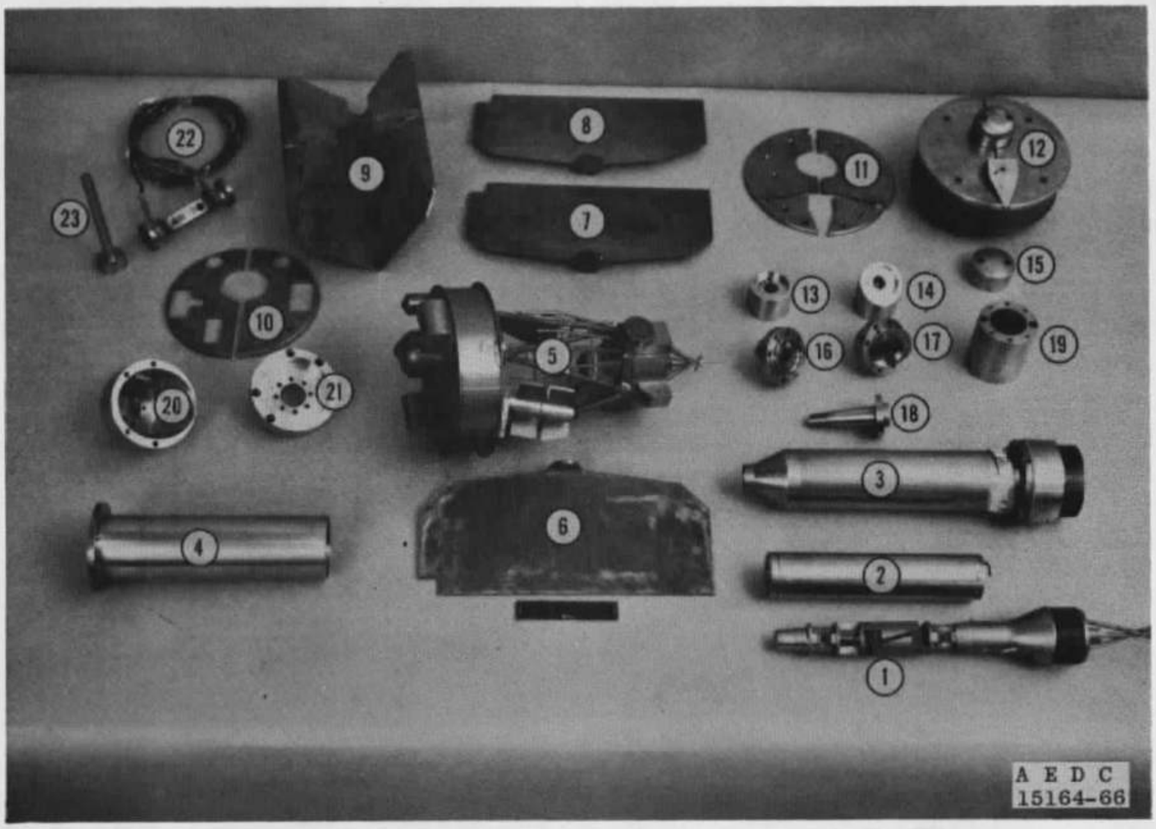

Item No.	Description
1	Six-Component 400-lb Balance
2	Balance Water Jacket
3-4	Windshields
5	Basic Nimbus Model with SNAP-19
6-7	Regular Solar Paddles
8	Modified Solar Paddle to Allow for Sting Clearance at ϕ_M = 90 deg
9	Folded Solar Paddles
10-11	Insulation Blankets
12	Sensory Ring (Snap-19 Shown on Item 5)
13-14	Prebend Adapters for Sensory Ring Only
15	Fuel Tank Dome for Sensory Ring
16-17	Prebend Adapters for Nimbus Control Housing
18	Water Jacket to Model Adapter
19	2.25-in.-Long Extension for Nimbus with Folded Solar Paddles
20-21	Prebend Adapters for Nimbus Sensory Ring
22	Instrumented Solar Paddle Support Beam for Obtaining Beam Bending Moments
23	Calibration Body for Item 22

b. Photograph Showing Model and Components

Fig. 1 Continued

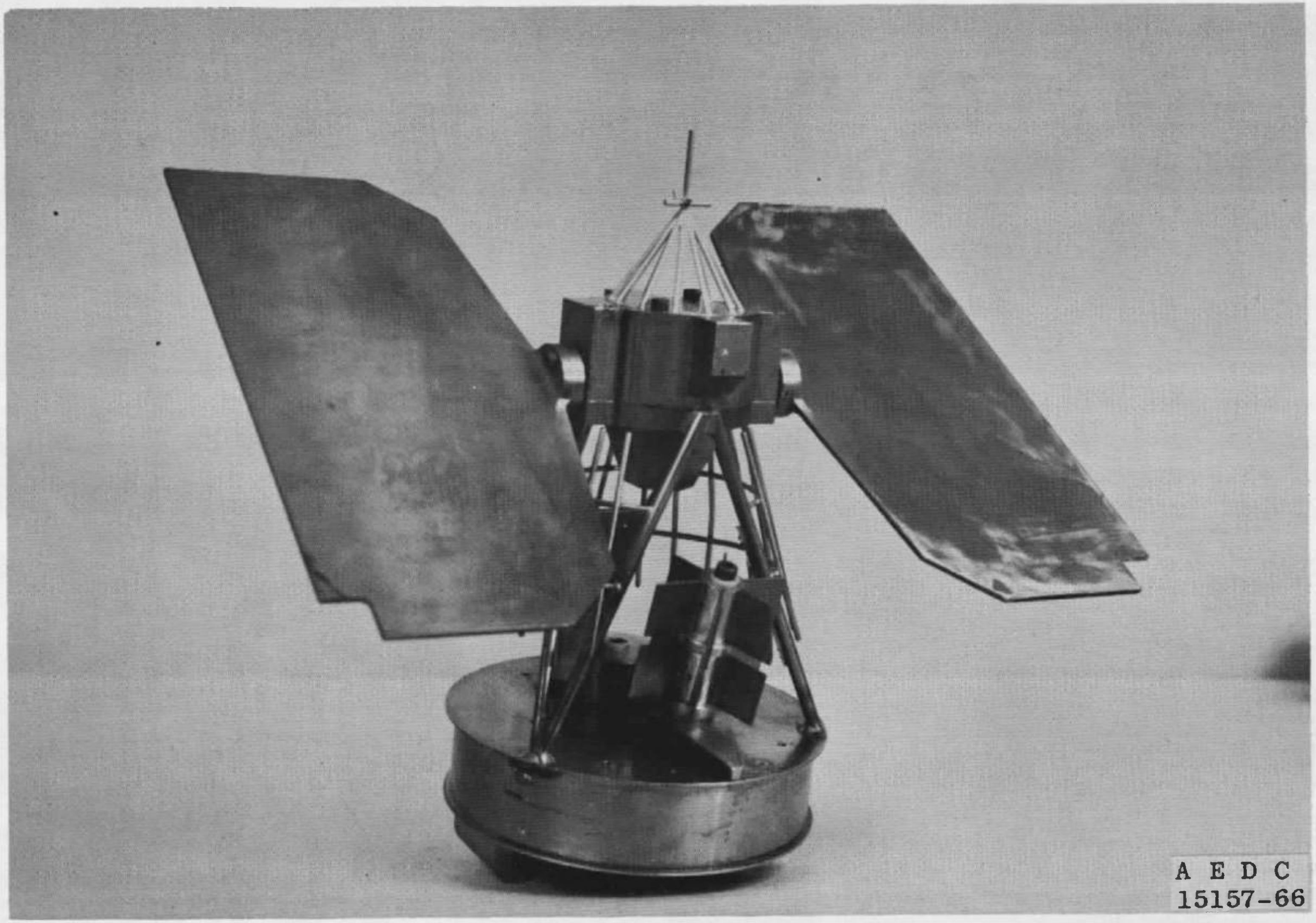

c. Photograph of Assembled Model, δ = 60 deg

Fig. 1 Continued

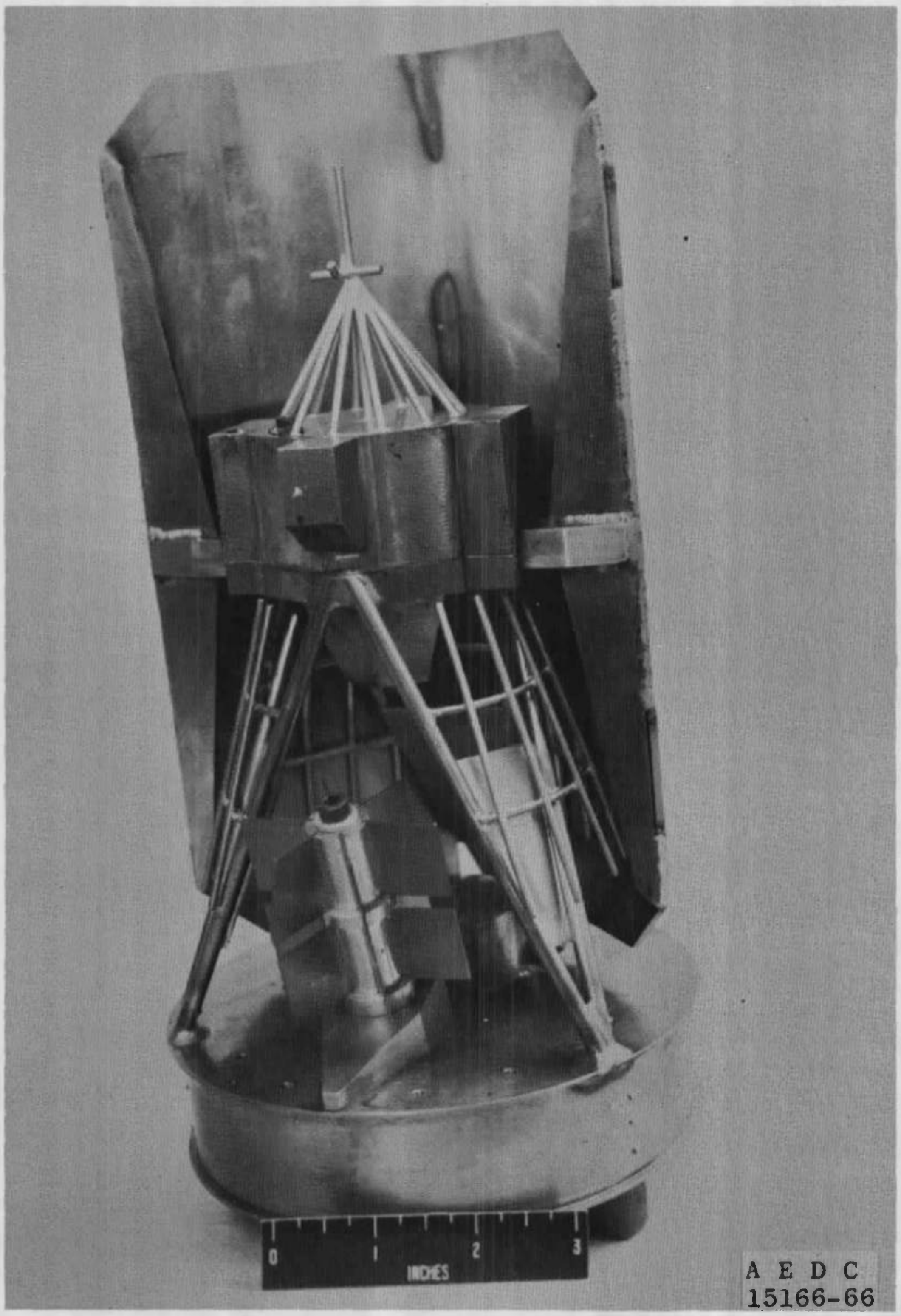

d. Photograph Showing the Solar Paddles Folded

Fig. 1 Continued

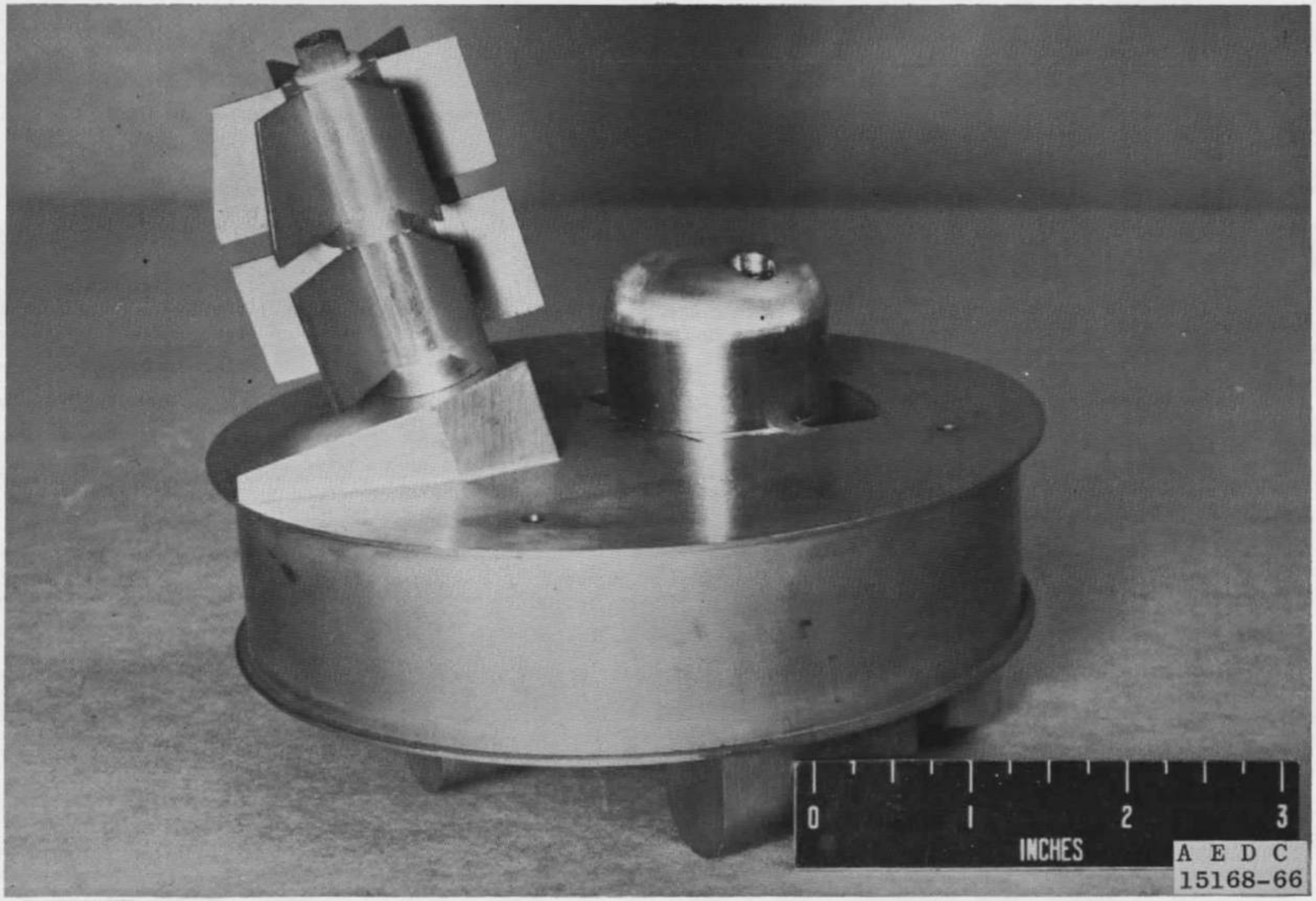

e. Photograph Showing Sensory Ring-SNAP-19 Configuration

Fig. 1 Concluded

Config.	R_1, in.	R_2, in.
1	2.58	3.18
2	1.77	3.18

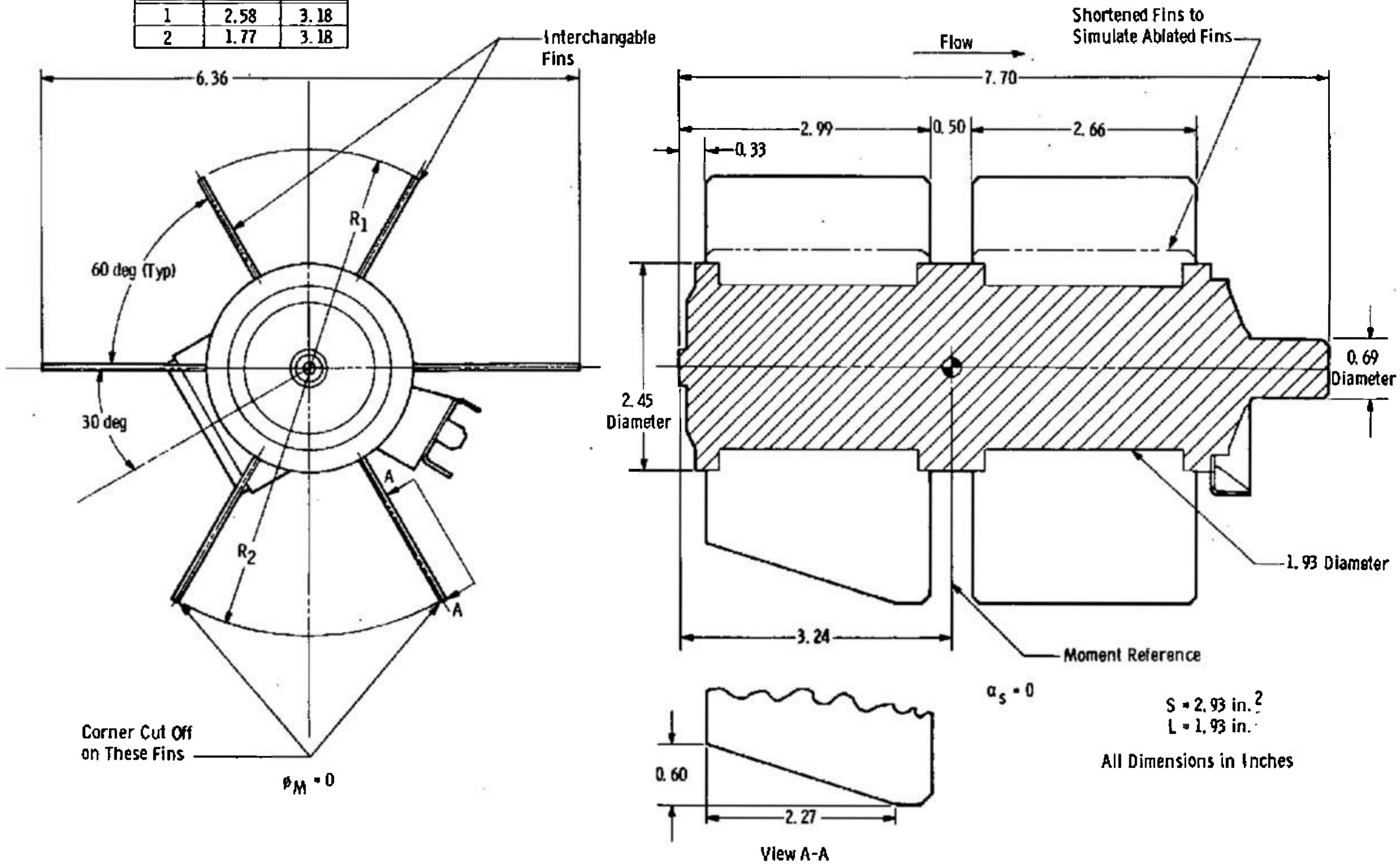

a. Model Details

Fig. 2 SNAP-19 Force Model

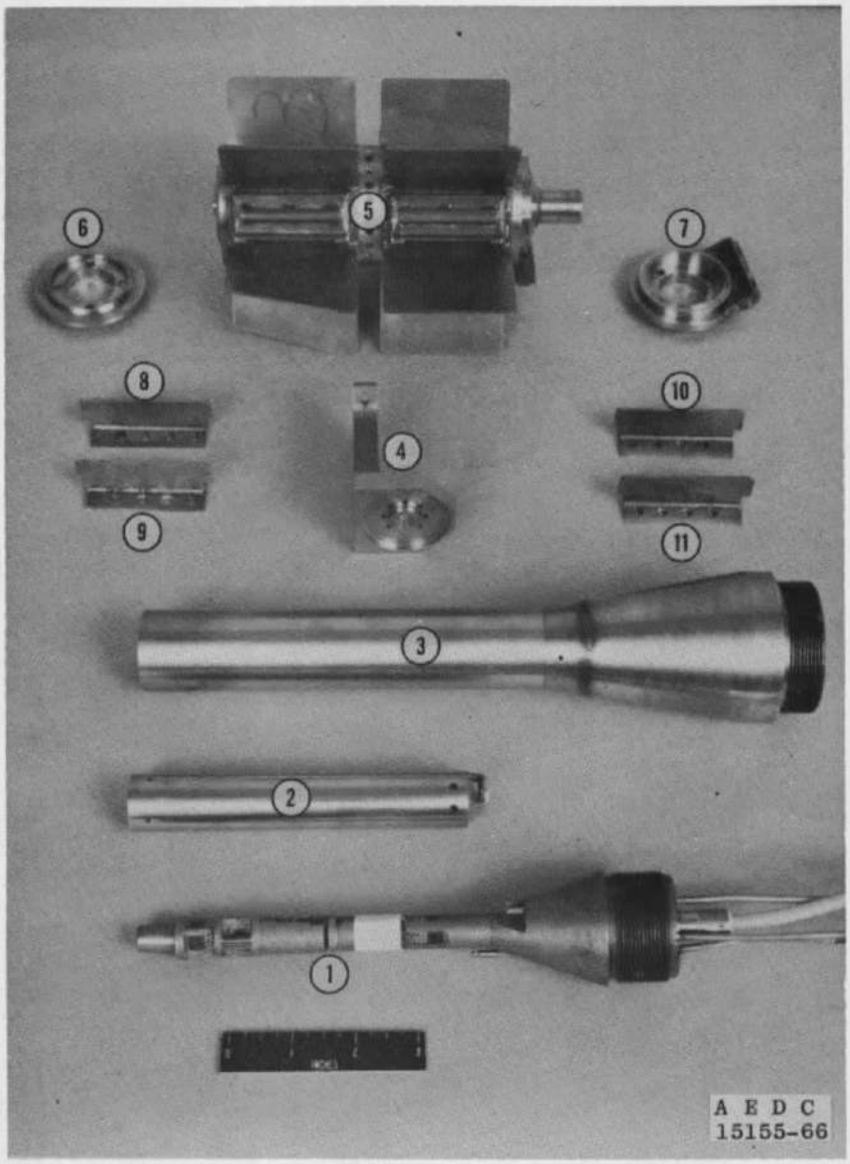

Item No.	Description
1	Six-Component 80-lb Balance
2	Balance Water Jacket
3	Windshield
4	90-deg Balance-Model Adapter
5	SNAP-19 Force Model
6	Model-Windshield Fairing for Forward End of Model
7	Model-Windshield Fairing for Aft End of Model
8-11	Interchangeable Fins

b. Photograph of Model and Components

Fig. 2 Concluded

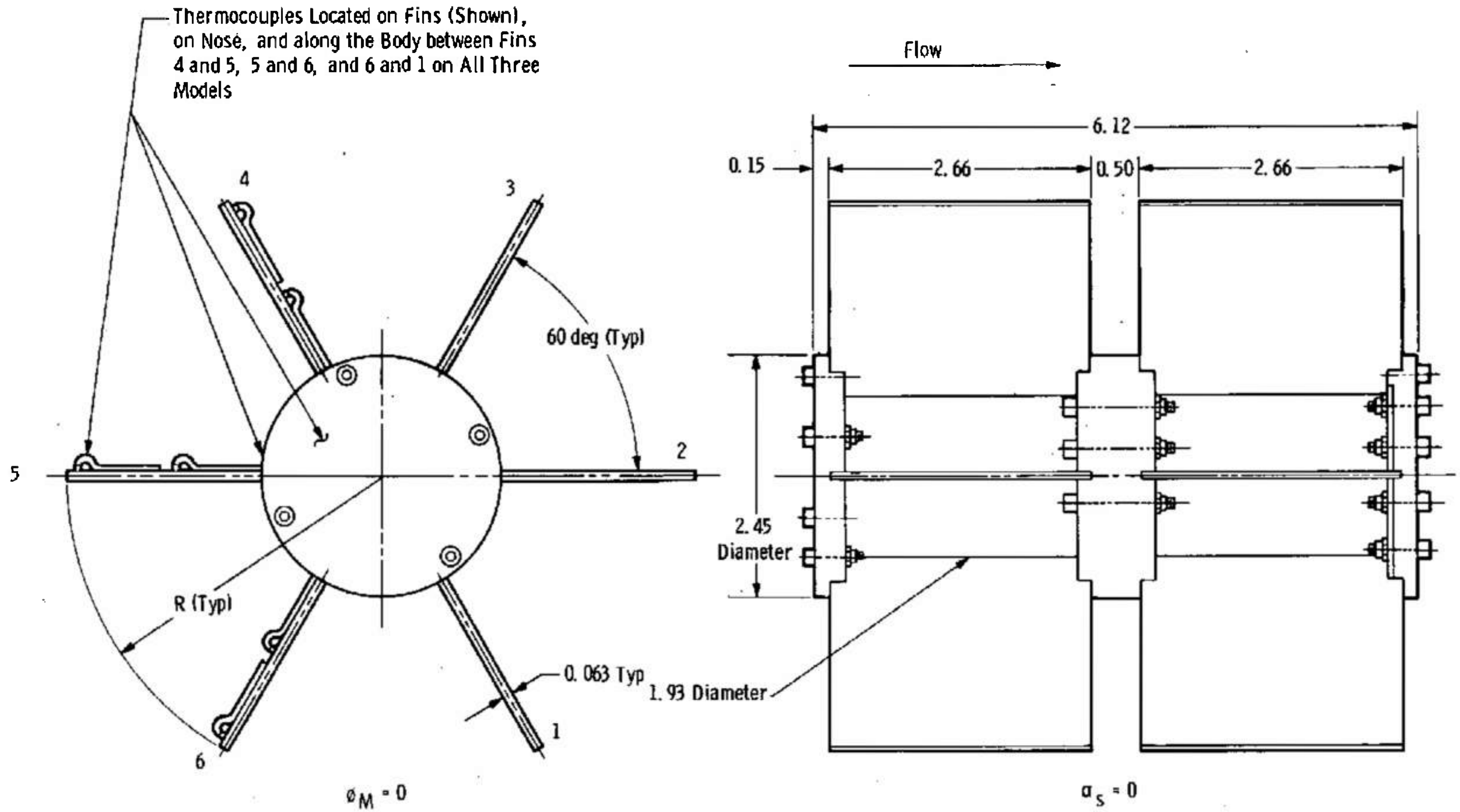

All Dimensions in Inches

Config.	1	2	3
R, in.	3.18	2.44	1.70
T/C's	98	98	78

0.050 Nominal Skin Thickness on Centerbody and Nose

a. Model Details

Fig. 3 SNAP-19 Heat-Transfer Models

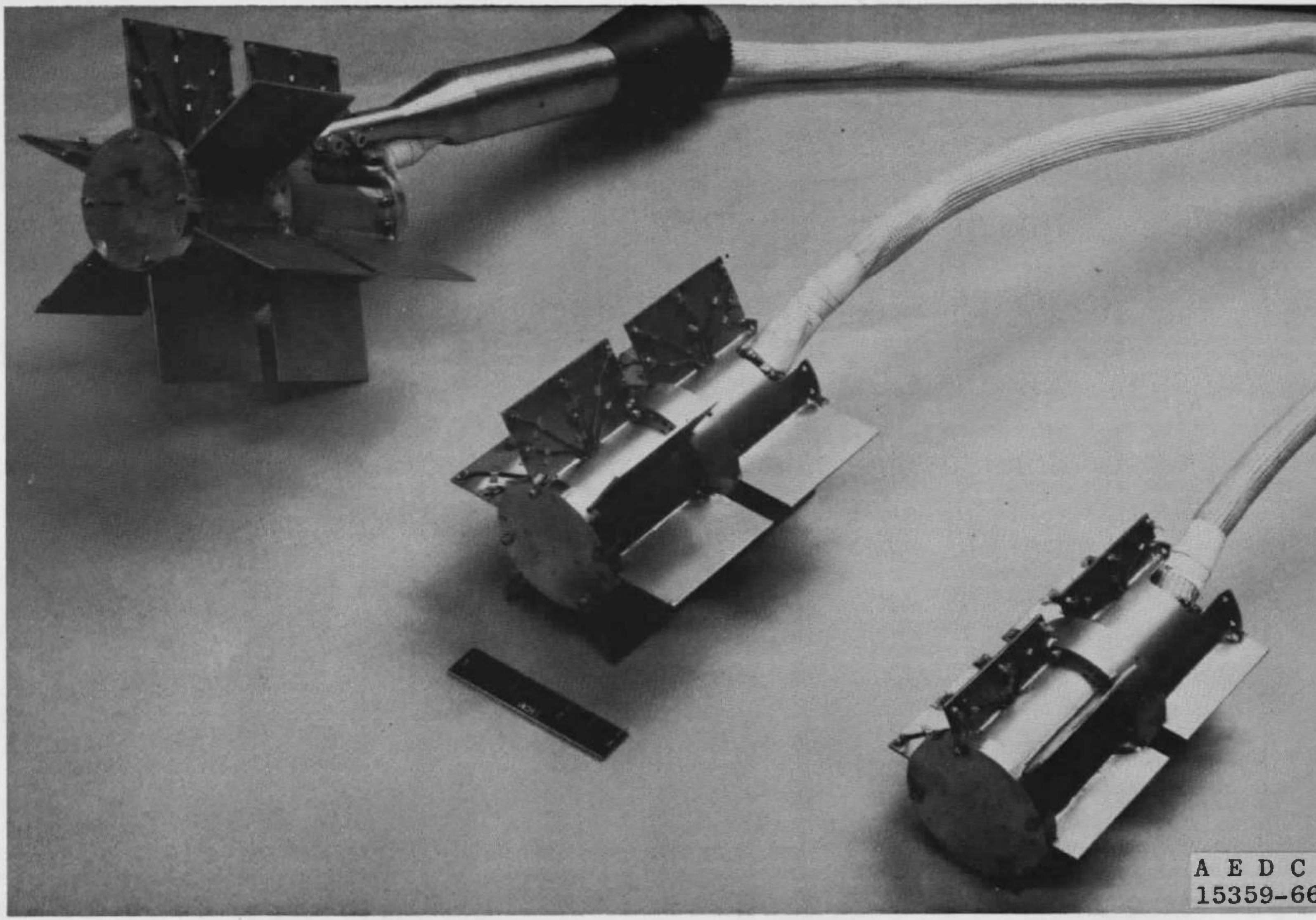

b. Photograph of Models

Fig. 3 Concluded

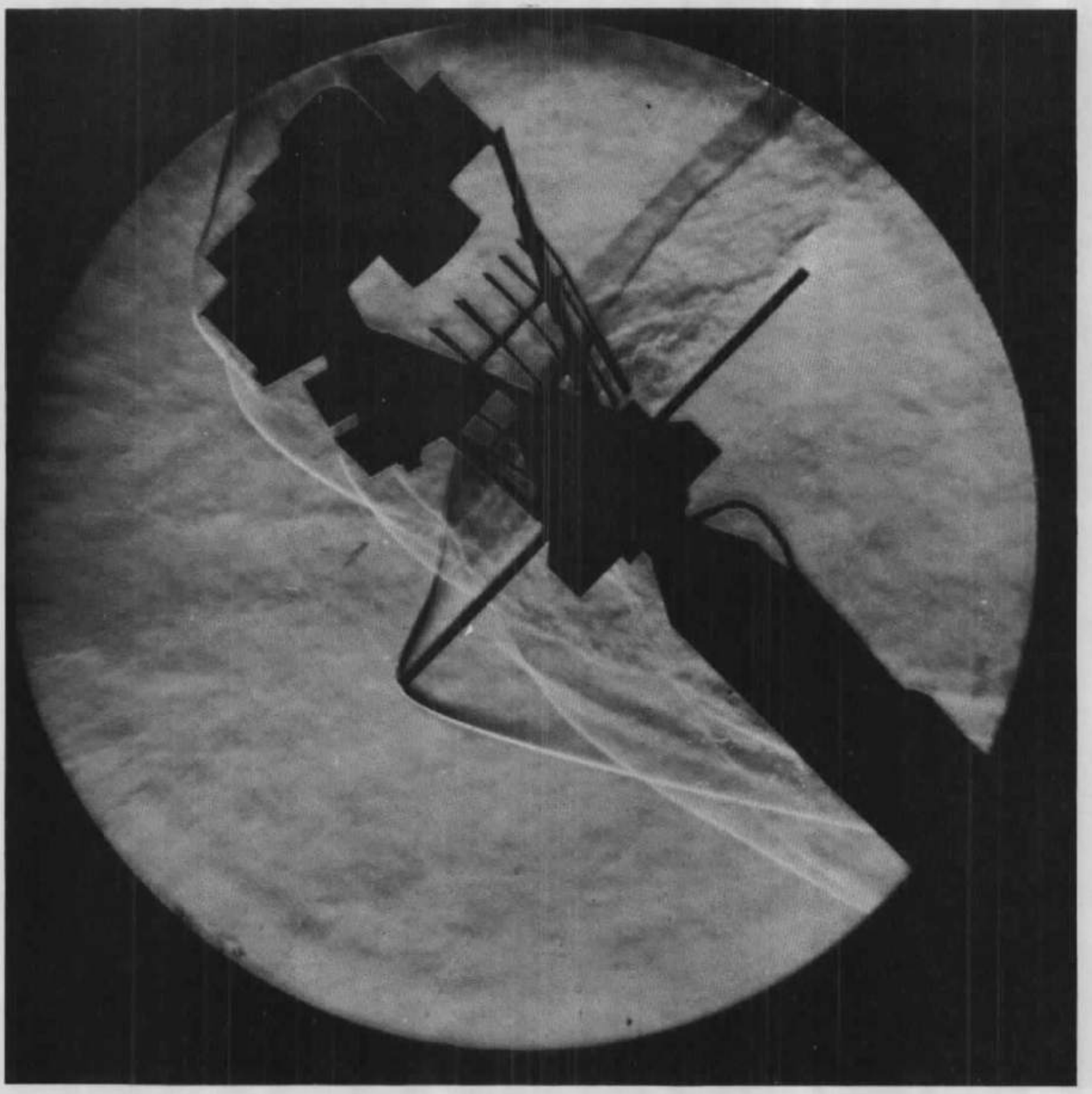

a. α_s = 45 deg, ϕ_M = 0, δ = +90 deg

Fig. 4 Typical Schlieren Photographs of Nimbus Model

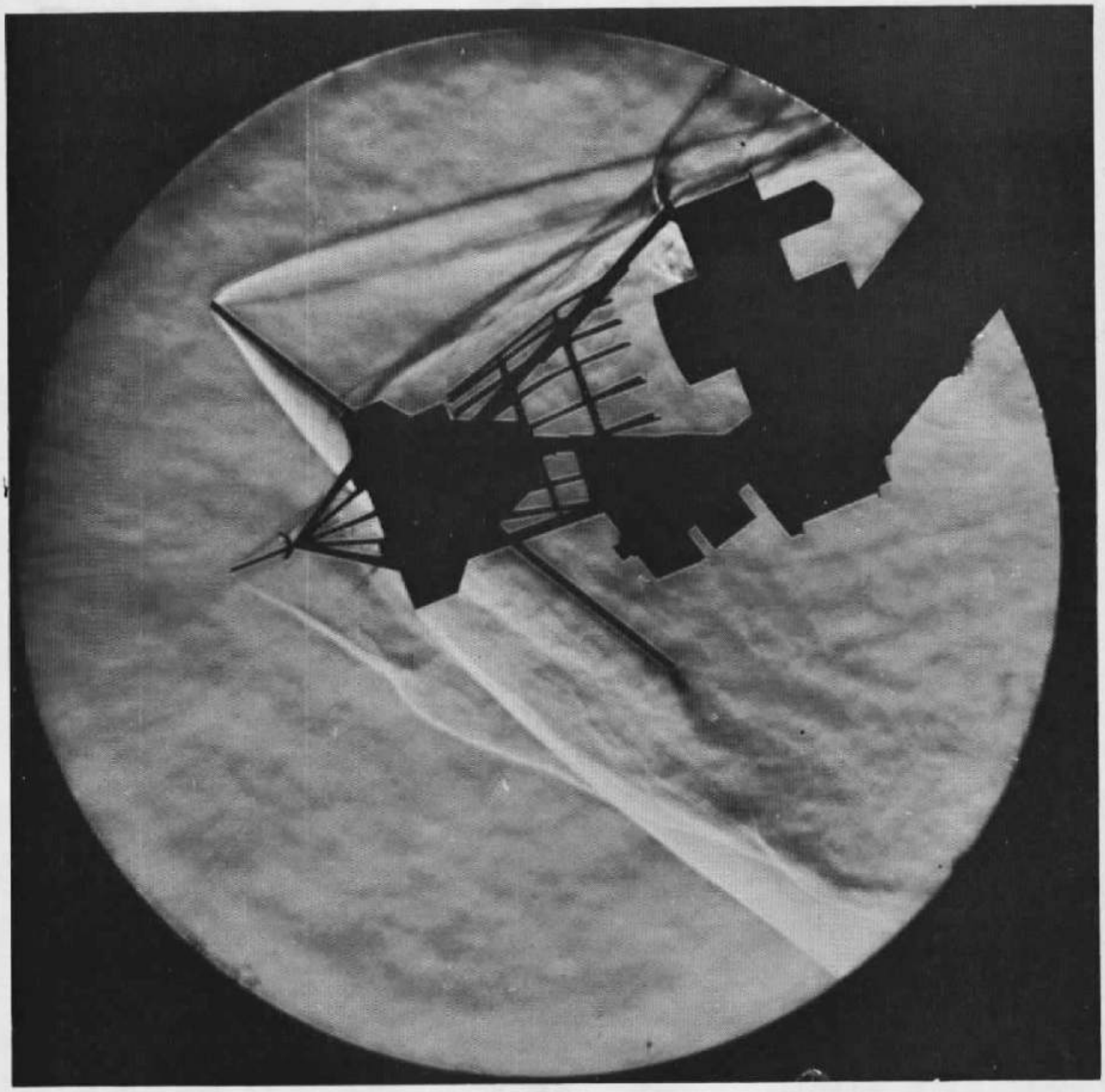

b. α_s = 159 deg, ϕ_M = 180 deg, δ = −60 deg
Fig. 4 Concluded

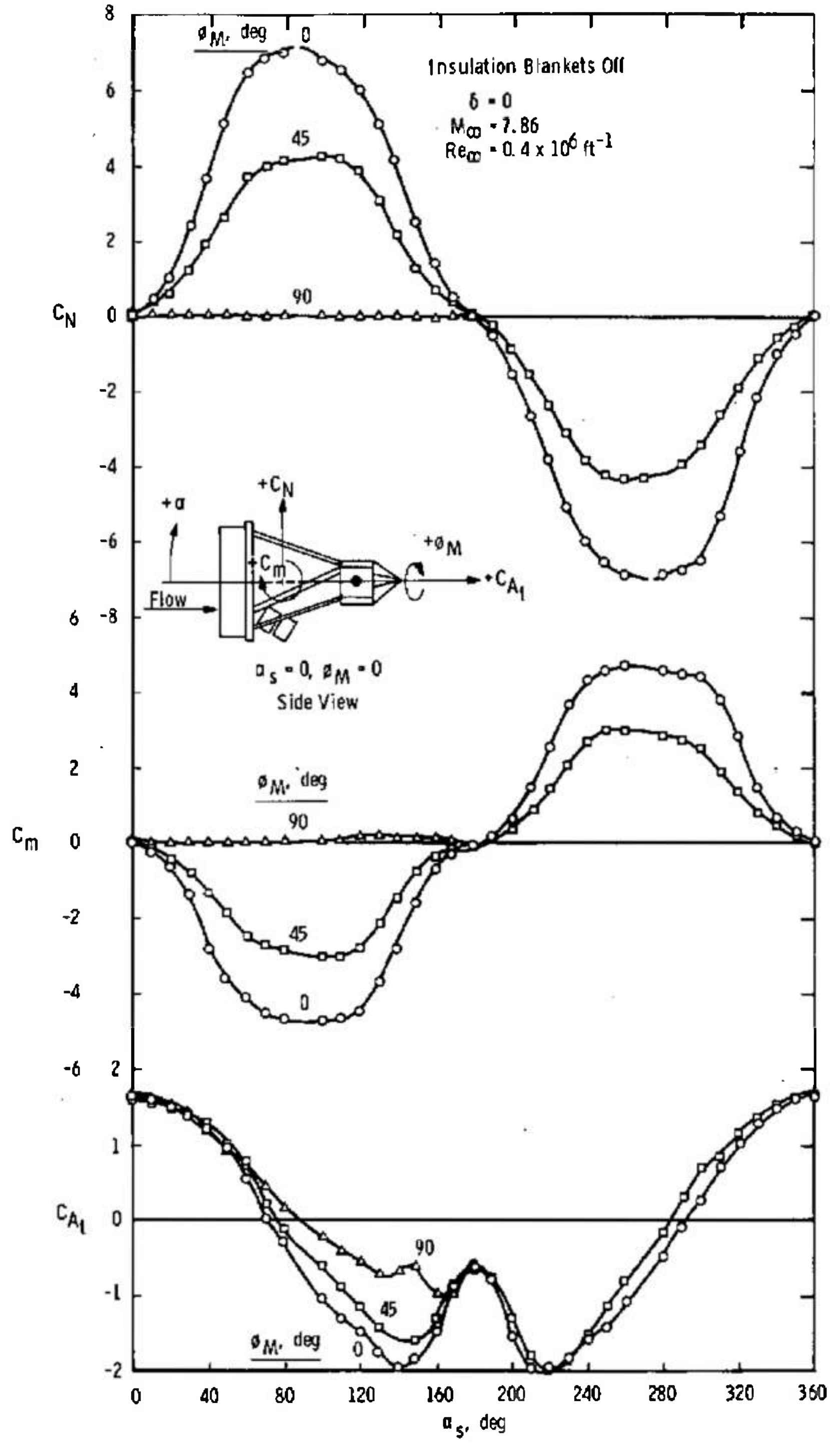

a. Longitudinal Stability and Axial Force

Fig. 5 Aerodynamic Characteristics of the Nimbus Spacecraft with Insulation Blankets Off, $\delta = 0$

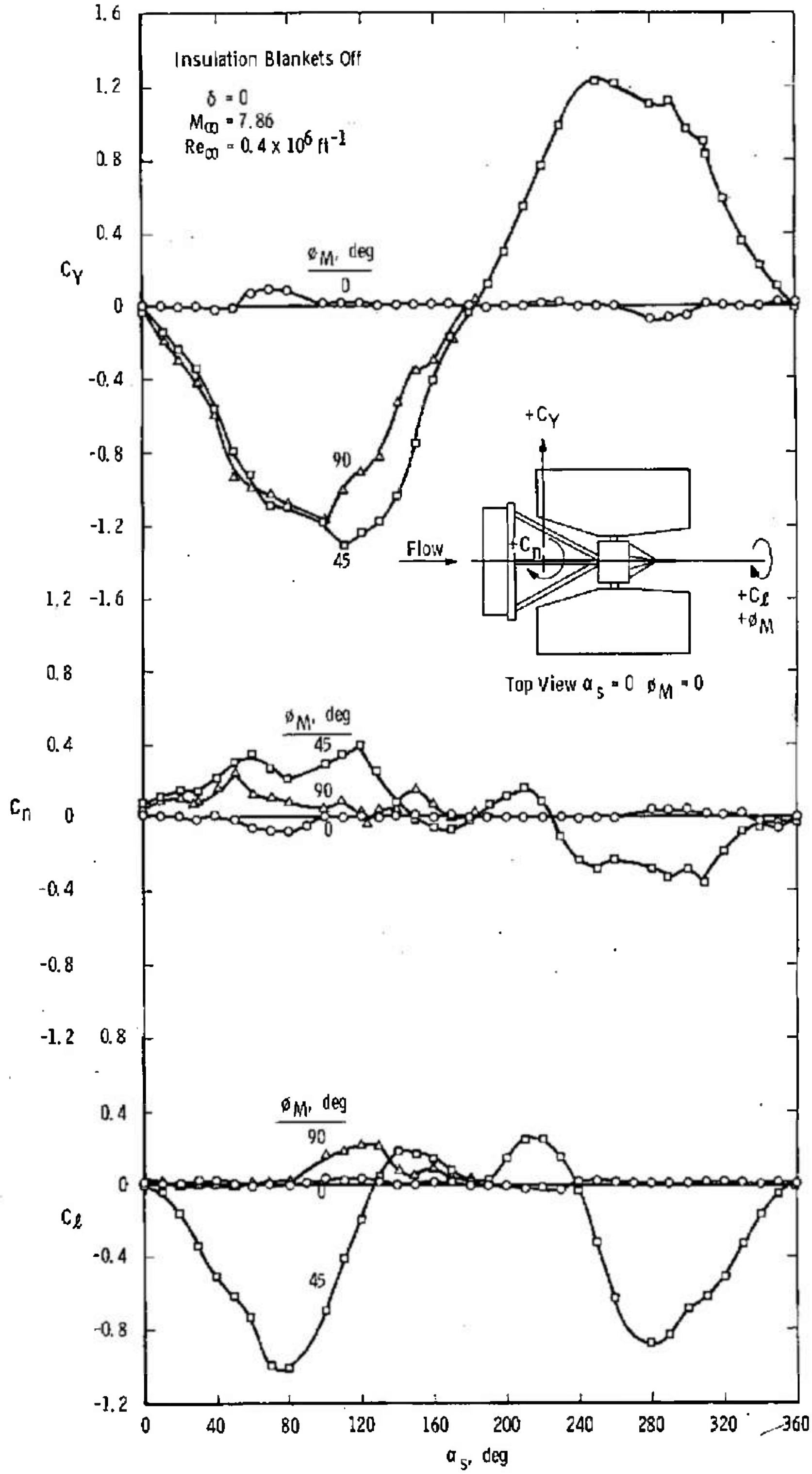

b. Lateral Stability and Rolling Moment

Fig. 5 Concluded

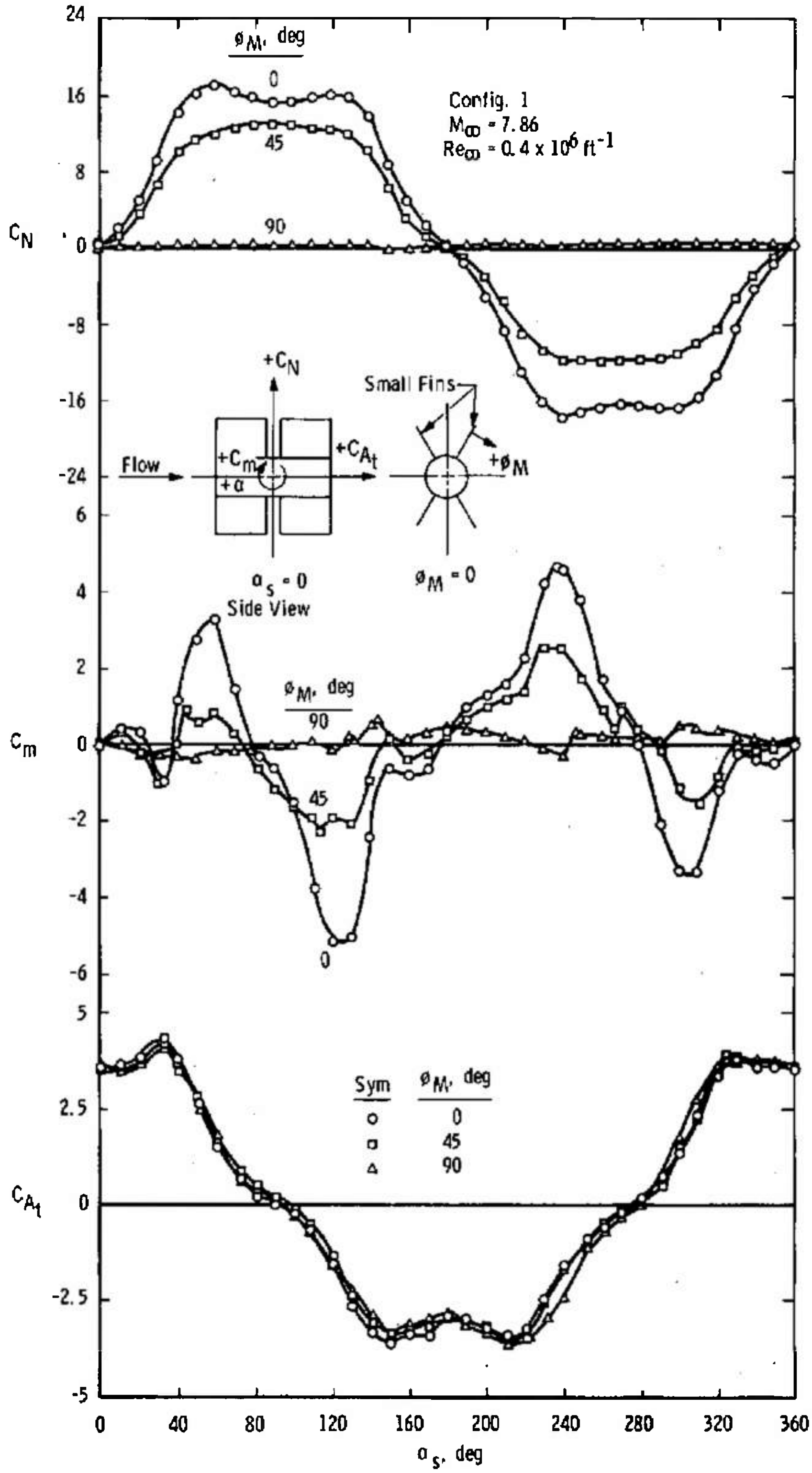

a. Longitudinal Stability and Axial Force

Fig. 6 Aerodynamic Characteristics of the SNAP-19 Generator with Nonablated Fins

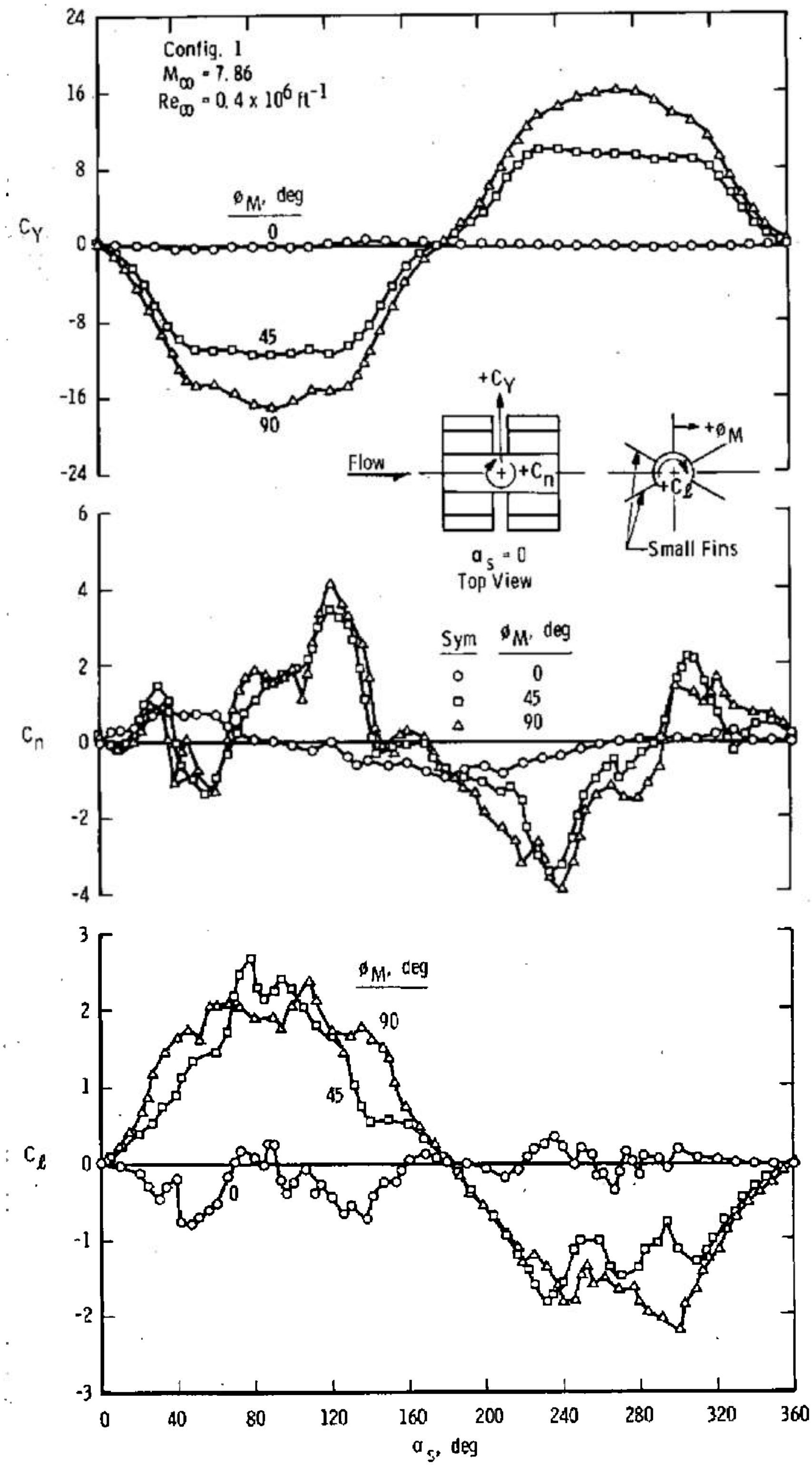

b. Lateral Stability and Rolling Moment

Fig. 6 Concluded

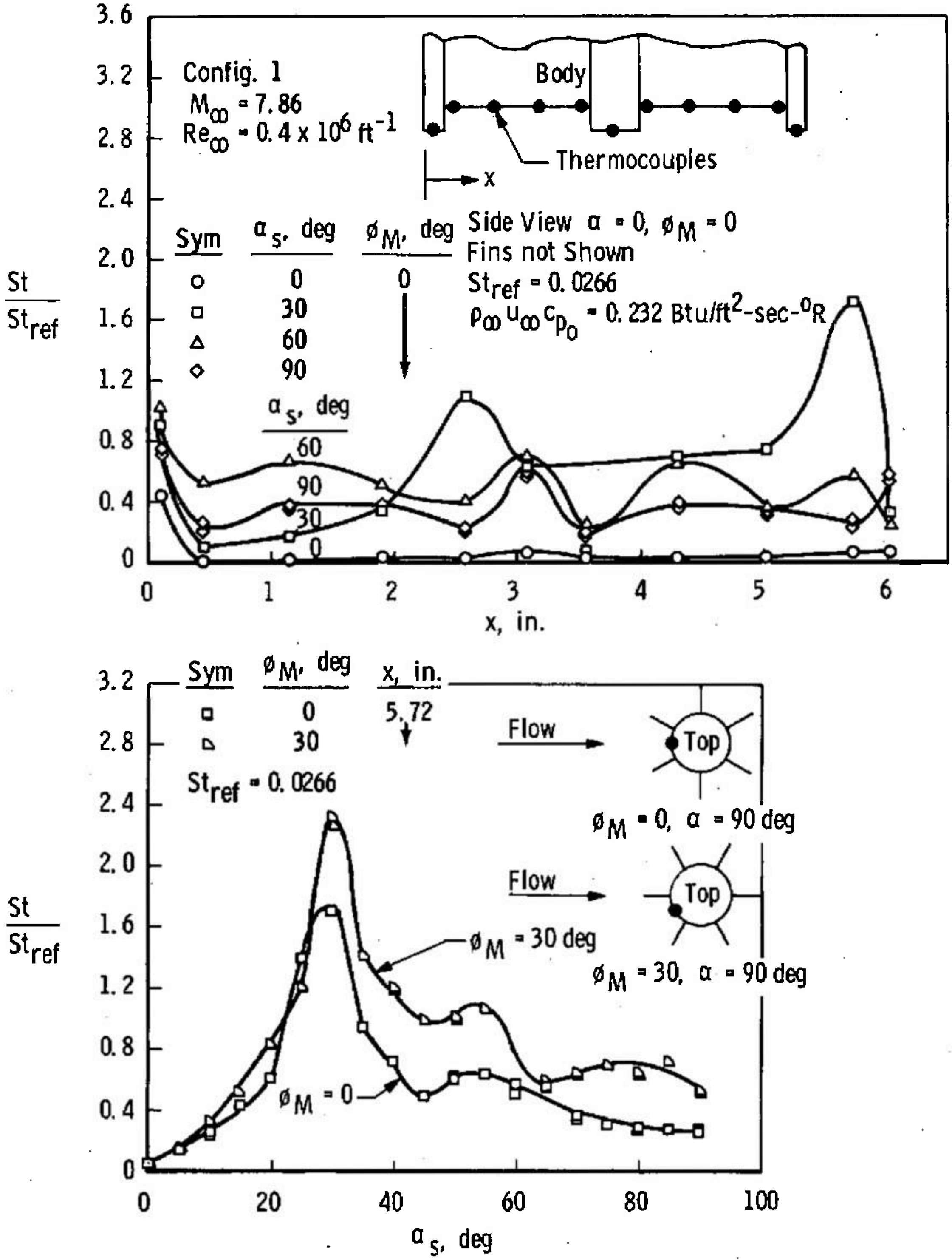

a. Centerbody

Fig. 7 Heat-Transfer Distributions on the SNAP-19 Generator with Nonablated Fins

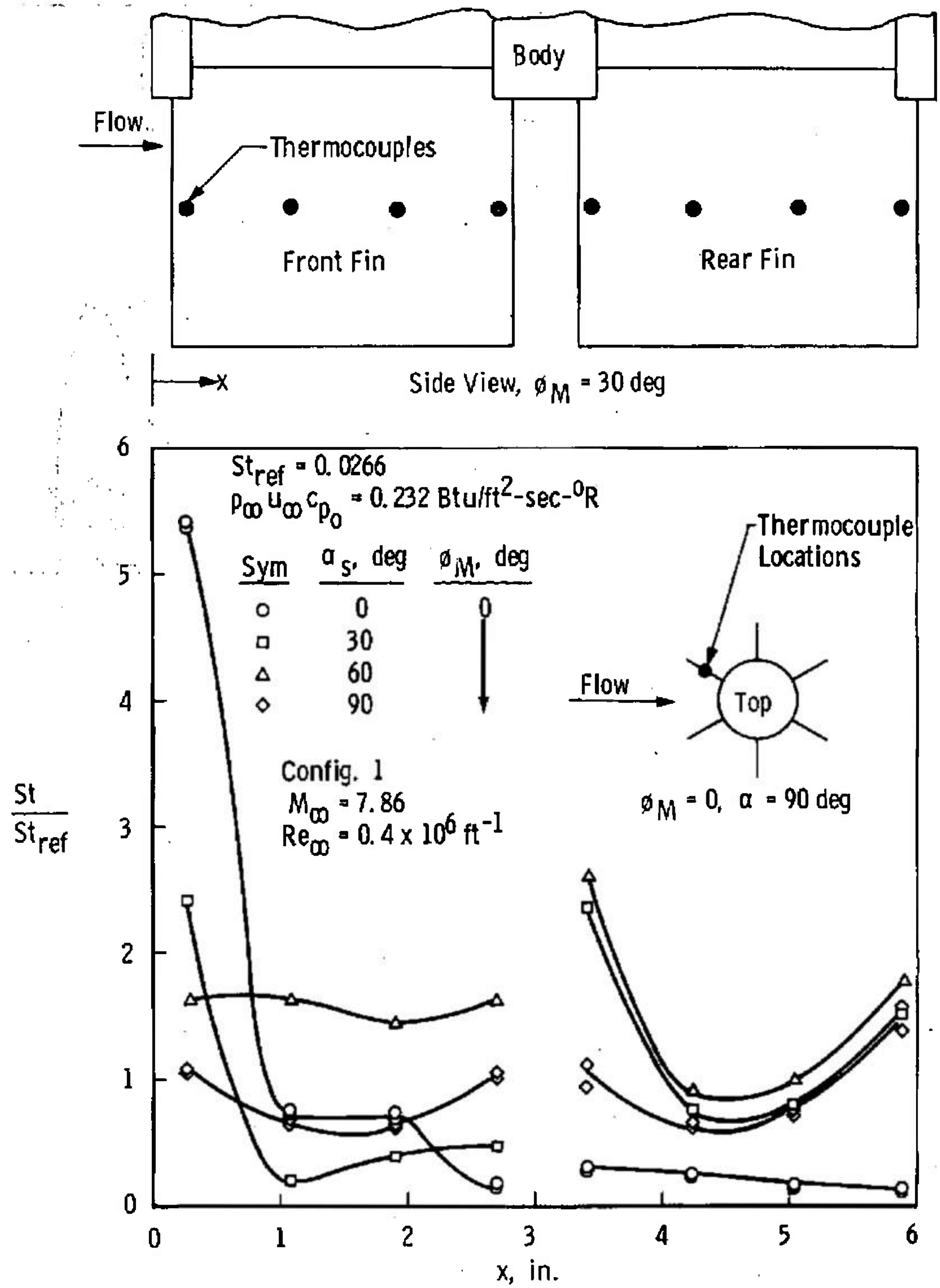

b. Fins

Fig. 7 Concluded

Security Classification

DOCUMENT CONTROL DATA - R&D

(Security classification of title, body of abstract and indexing annotation must be entered when the overall report is classified)

1. ORIGINATING ACTIVITY (Corporate author) Arnold Engineering Development Center (AEDC) ARO, Inc., Operating Contractor Arnold Air Force Station, Tennessee	2a. REPORT SECURITY CLASSIFICATION UNCLASSIFIED 2b. GROUP N/A

3. REPORT TITLE

MACH 8 AERODYNAMIC AND AEROTHERMODYNAMIC CHARACTERISTICS OF THE NIMBUS B SPACECRAFT AND SNAP-19 NUCLEAR GENERATOR

4. DESCRIPTIVE NOTES (Type of report and inclusive dates)

N/A

5. AUTHOR(S) (Last name, first name, initial)

Burt, R. H., ARO, Inc.

6. REPORT DATE	7a. TOTAL NO. OF PAGES	7b. NO. OF REFS
October 1966	31	1

8a. CONTRACT OR GRANT NO. AF40(600)-1200 b. AEC Activity No. 04-60-50-01.1 c. d.	9a. ORIGINATOR'S REPORT NUMBER(S) AEDC-TR-66-194 9b. OTHER REPORT NO(S) (Any other numbers that may be assigned this report) N/A

10. AVAILABILITY/LIMITATION NOTICES

~~Qualified requesters may obtain copies of this report from DDC and transmittal to foreign governments or foreign nationals must have prior approval of AEC.~~

11. SUPPLEMENTARY NOTES	12. SPONSORING MILITARY ACTIVITY
N/A	Atomic Energy Commission Albuquerque, New Mexico

13. ABSTRACT

Static-stability and axial-force characteristics were obtained on a 10-percent scale model of the Nimbus B spacecraft and on a 30-percent scale model of the SNAP-19 nuclear generator at angles of attack from 0 to 180 deg and model roll angles from 0 to 225 deg on the Nimbus and from -60 to 270 deg on the SNAP-19 models. Heat-transfer distributions were obtained on three 30-percent scale models of the SNAP-19 generator with various fin lengths to simulate fin ablation and at angles of attack from 0 to 90 deg and model roll angles of 0 and 30 deg. The tests were conducted at Mach 8 at a free-stream Reynolds number of 0.4 million per foot. Selected results are presented to illustrate the types of data obtained.

This document has been approved for public release its distribution is unlimited.

Per AF Letter dtd 23 January 75 signed William O. Cole.

DD FORM 1 JAN 64 1473

Security Classification

Security Classification

14. KEY WORDS	LINK A		LINK B		LINK C	
	ROLE	WT	ROLE	WT	ROLE	WT
SNAP-19						
Nimbus B						
aerothermodynamics						
spacecrafts						
4 nuclear generator						
stability						
force						
heat transfer						

16-12

1. Missiles -- Nimbus B
2. Nuclear reactors: Snap 19.
3. Nuclear vehicles.
5 Space vehicles -- Heat transfer
6 " " -- Performance

INSTRUCTIONS

1. ORIGINATING ACTIVITY: Enter the name and address of the contractor, subcontractor, grantee, Department of Defense activity or other organization *(corporate author)* issuing the report.

2*a*. REPORT SECURITY CLASSIFICATION: Enter the overall security classification of the report. Indicate whether "Restricted Data" is included. Marking is to be in accordance with appropriate security regulations.

2*b*. GROUP: Automatic downgrading is specified in DoD Directive 5200.10 and Armed Forces Industrial Manual. Enter the group number. Also, when applicable, show that optional markings have been used for Group 3 and Group 4 as authorized.

3. REPORT TITLE: Enter the complete report title in all capital letters. Titles in all cases should be unclassified. If a meaningful title cannot be selected without classification, show title classification in all capitals in parenthesis immediately following the title.

4. DESCRIPTIVE NOTES: If appropriate, enter the type of report, e.g., interim, progress, summary, annual, or final. Give the inclusive dates when a specific reporting period is covered.

5. AUTHOR(S): Enter the name(s) of author(s) as shown on or in the report. Enter last name, first name, middle initial. If military, show rank and branch of service. The name of the principal author is an absolute minimum requirement.

6. REPORT DATE: Enter the date of the report as day, month, year; or month, year. If more than one date appears on the report, use date of publication.

7*a*. TOTAL NUMBER OF PAGES: The total page count should follow normal pagination procedures, i.e., enter the number of pages containing information.

7*b*. NUMBER OF REFERENCES: Enter the total number of references cited in the report.

8*a*. CONTRACT OR GRANT NUMBER: If appropriate, enter the applicable number of the contract or grant under which the report was written.

8*b*, 8*c*, & 8*d*. PROJECT NUMBER: Enter the appropriate military department identification, such as project number, subproject number, system numbers, task number, etc.

9*a*. ORIGINATOR'S REPORT NUMBER(S): Enter the official report number by which the document will be identified and controlled by the originating activity. This number must be unique to this report.

9*b*. OTHER REPORT NUMBER(S): If the report has been assigned any other report numbers *(either by the originator or by the sponsor)*, also enter this number(s).

10. AVAILABILITY/LIMITATION NOTICES: Enter any limitations on further dissemination of the report, other than those imposed by security classification, using standard statements such as:

(1) "Qualified requesters may obtain copies of this report from DDC."

(2) "Foreign announcement and dissemination of this report by DDC is not authorized."

(3) "U. S. Government agencies may obtain copies of this report directly from DDC. Other qualified DDC users shall request through

_______________________________."

(4) "U. S. military agencies may obtain copies of this report directly from DDC. Other qualified users shall request through

_______________________________."

(5) "All distribution of this report is controlled. Qualified DDC users shall request through

_______________________________."

If the report has been furnished to the Office of Technical Services, Department of Commerce, for sale to the public, indicate this fact and enter the price, if known.

11. SUPPLEMENTARY NOTES: Use for additional explanatory notes.

12. SPONSORING MILITARY ACTIVITY: Enter the name of the departmental project office or laboratory sponsoring *(paying for)* the research and development. Include address.

13. ABSTRACT: Enter an abstract giving a brief and factual summary of the document indicative of the report, even though it may also appear elsewhere in the body of the technical report. If additional space is required, a continuation sheet shall be attached.

It is highly desirable that the abstract of classified reports be unclassified. Each paragraph of the abstract shall end with an indication of the military security classification of the information in the paragraph, represented as *(TS)*, *(S)*, *(C)*, or *(U)*.

There is no limitation on the length of the abstract. However, the suggested length is from 150 to 225 words.

14. KEY WORDS: Key words are technically meaningful terms or short phrases that characterize a report and may be used as index entries for cataloging the report. Key words must be selected so that no security classification is required. Identifiers, such as equipment model designation, trade name, military project code name, geographic location, may be used as key words but will be followed by an indication of technical context. The assignment of links, rules, and weights is optional.

Security Classification